Supporting Information for

Discovery and Characterization of a Naturally Occurring, Turn-on Yellow Fluorescent Protein Sensor for Chloride

Jasmine N. Tutol[§,†], Weicheng Peng[§,‡], and Sheel C. Dodani[†*]

[†]Departments of Chemistry and Biochemistry and [‡]Biological Sciences, The University of Texas at Dallas, Richardson, Texas 75080, United States

*E-mail: sheel.dodani@utdallas.edu

METHODS

General. Reagents and chemicals were purchased from Sigma-Aldrich (St. Louis, MO) or Thermo Fisher Scientific (Waltham, MA) and were used as received unless otherwise stated.

Sequence alignment, percent identity matrix, and crystal structures. Sequences were aligned using the Clustal Omega software v1.2.4.[1] The percent identity matrix was generated using the Clustal Omega software v2.1.[1] Crystal structures in Figure 1 were generated using MacPyMol v1.7 (Schrödinger, LLC, New York City, NY).

Plasmid and site-saturation mutagenesis library construction. The genes encoding the wild-type yellow fluorescent protein from *Phialidium sp.* (phiYFP, UniProt ID: Q6RYS7) and the yellow fluorescent protein H148Q from *Aequorea victoria* (avYFP-H148Q, UniProt ID: P42212) were codon optimized for *Escherichia coli* K12 using the Integrated DNA Technologies Codon Optimization Tool. The genes were cloned into the pET-28b(+) vector between the Nde1 and BamH1 restriction sites with an N-terminal polyhistidine-tag and a C-terminal stop codon (Figure S23, GenScript, Piscataway, NJ).

Site-saturation mutagenesis (SSM) was carried out as previously described with the phiYFP template at position Q69.[2,3] A 100 µM solution of three forward primers, each 37 bases long and containing the degenerate base triplet NDT, VHG, and TGG at the Q69-position were mixed in a 12:9:1 ratio and diluted to a final concentration of 10 µM with autoclaved water (Sigma-Aldrich, St. Louis, MO). The reverse primer, 34 bases long with 18 bases overlapping with the forward primer (Table S2), was also diluted to 10 µM with autoclaved water. The polymerase chain reaction (PCR) was carried out with 1µL of the 10 ng/µL template plasmid stock solution, 1.5 µL of the 10 µM forward and reverse primer stock solutions, 0.5 µL of the 10 mM deoxynucleotides (dNTPs) stock solution, 0.5 µL of DMSO, 5 µL of 5X Phusion GC buffer, 0.25 µL of Phusion DNA polymerase, and 14.8 µL of autoclaved water to a final volume of 25 µL at 54.5 °C annealing temperature (Table S3) according to manufacturer's directions (Phusion High Fidelity PCR Kit, catalog number: M0530; New England Biolabs, Ipswich, MS). After the PCR was complete, the template DNA was removed with 1 µL *Dpn1* (catalog number: R0176L; New England Biolabs, Ipswich, MS) for 2 h at 37 °C. The PCR product was then separated with agarose gel electrophoresis, extracted, and purified with the Zymoclean Gel DNA Recovery Kit (catalog number: D4002; Zymo Research, Irvine, CA). The concentration of the purified PCR product was determined using the NanoDrop™ Lite Spectrophotometer (catalog number: NDNDLUSCAN; Thermo Fisher Scientific, Waltham, MA). One hundred nanograms of the DNA was recircularized for 1 h at 50 °C using 10 µL of the Gibson Assembly Master Mix (catalog number: E2611L; New England Biolabs, Ipswich, MS) diluted to a final volume of 20 µL in autoclaved water. The reaction product was isolated with the DNA Clean & Concentrator Kit (catalog number: D4004; Zymo Research, Irvine, CA).

Library expression, screening, and validation. The SSM library plasmid prepared above was used to transform electrocompetent *E. cloni* EXPRESS BL21 (DE3) Competent Cells (catalog number: 60300; Lucigen, Middleton, WI) with a MicroPulser Electroporator (catalog number: 1652100; Bio-Rad Laboratories, Hercules, CA) according to manufacturer's instructions. Cells containing a plasmid were selected using Luria Broth (LB; catalog number: L24040500, Research Products International, Mount Prospect, IL) agar plates containing 30 µg/mL kanamycin sulfate and incubated overnight at 37 °C (New Brunswick Innova 42R Shaker; catalog number: M13350014; Eppendorf, Hamburg, Germany). For library expression, 88 single colonies and 8 single colonies of wild-type phiYFP were picked into 500 µL of LB containing 30 µg/mL kanamycin sulfate in a 96-deep-well plate (catalog number: 780280; Greiner Bio-One, Kremsünster, Austria) and sealed with an EasyApp microporous film (catalog number: 2978-5872; USA Scientific, Ocala, FL). The 96-deep-well plate was incubated for 18 h at 37 °C with shaking at 250 rpm. The following day, 50 µL of the overnight culture was used to inoculate another 96-deep-well plate filled with 950 µL of LB containing 30 µg/mL kanamycin sulfate with a Biomek NX^P liquid handler (catalog number: A31841; Beckman Coulter, Brea, CA) and incubated for 3 h at 37 °C with shaking at 250 rpm. Protein expression was induced with the addition of 50 µL of LB containing 30 µg/mL kanamycin sulfate and 21 mM isopropyl beta-D-thiogalactopyranoside (IPTG, catalog number: I2481C50; Gold

Biotechnology, Olivette, MO) to each well for a final concentration of 1 mM IPTG and carried out for 24 h at 37 °C with shaking at 250 rpm. After 24 h, the cells were harvested by centrifugation at 2500*g* for 5 min (5810 R, catalog number: 2231000382; Eppendorf, Hamburg, Germany), the media was removed, and the cell pellets were stored at -20 °C overnight.

The frozen cell pellets were thawed for 30 min at room temperature, and then resuspended in 300 µL of 50 mM HEPES buffer (pH 8) containing 2 mg/mL lysozyme, 20 µg/mL deoxyribonuclease I, and 2 mM magnesium chloride by vortexing (Vortex 2 Shaker, catalog number: 0025001607; IKA Works, Staufen, Germany) with a VG 3.3 Universal attachment (catalog number: 0003342400; IKA Works, Staufen, Germany) and a VG 3.37 microtiter plate attachment (catalog number: 0003344400; IKA Works, Staufen, Germany). The cell lysis proceeded for 6 h at 37 °C with shaking at 250 rpm. The following day, the lysate was clarified by centrifugation at 3,000*g* for 1 h, and 25 µL of the supernatant was transferred to two 96-well microtiter plates (catalog number: 222-8050-F1K; Evergreen Scientific, Rancho Dominguez, CA) using the Biomek NX^{P} liquid handler. Each plate was diluted with either 175 µL of 50 mM sodium citrate buffer (pH 4.75) or 50 mM sodium citrate buffer (pH 4.75) containing 457 mM sodium chloride for a final concentration of 400 mM sodium chloride and a final pH ~ 5 using a multichannel pipette (Xplorer, catalog number: 486100148; Eppendorf, Hamburg, Germany) prior to scanning. For each well, the absorbance spectra were collected from 300 nm to 600 nm with 5 nm step size, followed by excitation at 400 nm, and the emission was collected from 500 nm to 600 nm with 5-nm step size, 30 flashes, and gain of 100 on a plate reader (Spark® 10M, catalog number: 30086376; Tecan, Männedorf, Switzerland).

Variants which maintained a similar level of fluorescence intensity to wild-type phiYFP and showed no significant response in the presence of 400 mM of sodium chloride were restreaked from the overnight source plate onto fresh LB agar plates containing 30 µg/mL kanamycin sulfate and incubated overnight at 37 °C. A single colony of each variant was picked into 5 mL of LB containing 30 µg/mL of kanamycin sulfate in a 14 mL culture tube (Falcon™ Round-Bottom Polystyrene Tube, catalog number: 352057; Corning Inc., Corning, NY) and incubated overnight at 37 °C with shaking at 250 rpm. The following day, 1 mL of the overnight cultures was diluted into 25 mL of 2xYT media containing 30 µg/mL kanamycin sulfate in 250 mL baffled flasks and incubated at 37 °C with shaking at 250 rpm. After 2 h, protein expression was induced at OD_{600} ~0.6-0.8 with 250 µL of 0.1 M IPTG for a final concentration 1 mM IPTG and carried out for 24 h at 37 °C with shaking at 250 rpm. Each expression culture was aliquoted to three 14-mL tubes and collected by centrifugation at 2,500*g* for 5 min. The resulting cell pellets were resuspended in 1 mL of 50 mM sodium citrate buffer (pH 5), 50 mM 2-(N-morpholino)ethanesulfonic acid (MES) buffer (pH 6), or 50 mM 3-(N-morpholino)propanesulfonic acid (MOPS) buffer (pH 7) and transferred to 1.5 mL microcentrifuge tubes (Seal Rite, catalog number: 1615-5500; USA Scientific). Cell lysis was carried out using sonication at 40% amplitude, 20 s pulse on, and 20 s pulse off for 1 min and 40 s (Q500, catalog number: Q500100; QSonica, Newtown, CT), and then the lysate was clarified by centrifugation at 5,000*g* for 10 min (5424 R, catalog number: 5404000537; Eppendorf, Hamburg, Germany). In a 96-well microtiter plate, 25 µL of the clarified lysate was diluted with 175 µL of the corresponding buffer or buffer containing 457 mM sodium chloride. For each well, absorbance and emission spectra were collected as described above. After the rescreen, variants that did not show a response to chloride at pH 5, 6, and 7 were picked into 5 mL of LB containing 30 µg/mL of kanamycin sulfate in 14 mL culture tubes and incubated overnight at 37 °C as described above. The following day, the cells were collected by centrifugation at 2,500*g* for 5 min and stored at -20 °C. The plasmid DNA was extracted using the QIAprep Spin Miniprep Kit (catalog number: 27106; Qiagen, Hilden, Germany) according manufacturer's instructions. The variants were sequenced to identify the single-point mutation (Eurofins Scientific, Louisville, KY).

Large-scale protein expression and purification. Plasmids encoding the wild-type phiYFP and Q69 variants and avYFP-H148Q were used to freshly transform *E. cloni*® EXPRESS BL21(DE3) Competent Cells (catalog number: 60300; Lucigen, Middleton, WI) as described above. Single colonies were picked into 25 mL 2xYT media containing 30 µg/mL kanamycin sulfate in 125 mL baffled flasks and incubated overnight at 37 °C with shaking at 230 rpm. Overnight cultures were diluted 1:50 in 300 mL of 2xYT containing 30 µg/mL kanamycin sulfate in 1 L baffled flasks and incubated at 37 °C for 2 h to OD_{600} ~0.6-

0.8. Protein expression was induced with 30 μL of 100 mM IPTG stock solution for a final concentration of 10 mM IPTG and carried out at 37 °C for 24 h with shaking at 230 rpm. The cells were then collected by centrifugation at 3,000*g* for 30 min at 4 °C, resuspended in 25 mL of 20 mM Tris buffer (pH 7.5) containing 200 mM sodium chloride, 5 mM magnesium chloride, and 30 μg/mL deoxyribonuclease I, and stored at -20 °C overnight.

The cell pellet was thawed for 30 min at room temperature and lysed using sonication at 30% amplitude, 15 s pulse on, and 45 s pulse off for 6 min. The lysate was clarified by ultracentrifugation at 18,000 rpm (Sorvall™ WX 80+, catalog number: 75000080; Thermo Fisher Scientific, Waltham, MA) for 25 min at 4 °C, and the supernatant was loaded into a 90 mL sample loop (DynaLoop 90, catalog number: 7500476; Bio-Rad Laboratories, Hercules, CA). Prior to sample loading, a 1 mL nickel nitrilotriacetic acid (Ni-NTA) affinity column (HisTrap™, catalog number: 17-5248-02; GE Healthcare, Little Chalfont, United Kingdom) was equilibrated with 10 column volumes (CV) of 50 mM MOPS running buffer (pH 7.5) containing 100 mM sodium chloride and 10 mM imidazole using the NGC™ Quest 10 Chromatography System (catalog number: 7880001; Bio-Rad Laboratories, Hercules, CA). The clarified lysate was loaded onto the equilibrated Ni-NTA column with a 1 mL/min flow rate. The column was washed with 20 CV of 50 mM MOPS running buffer (pH 7.5) containing 100 mM sodium chloride, and 10 mM imidazole. The polyhistidine-tagged protein was eluted with a 0% to 100% gradient of the running buffer and 50 mM Tris elution buffer (pH 7.5) containing 100 mM sodium chloride, and 500 mM imidazole over 20 CV and 100% of the elution buffer for 10 CV. Fractions with an absorbance 280 nm and 400 nm were pooled and buffer exchanged three times into 20 mM MOPS (pH 7.5) with an EMD Millipore Amicon™ Ultra-15 Centrifugal Filter Unit with a 10 kDa molecular weight cut-off (catalog number: UFC901024; MilliporeSigma, Burlington, MA) and stored at 4 °C until further use.

Protein concentration and extinction coefficient determination. The concentrations of purified wild-type phiYFP and variants and avYFP-H148Q were determined with the ThermoScientific™ Pierce™ Coomassie (Bradford) Protein Assay Kit (catalog number: PI23200; Thermo Fisher Scientific, Waltham, MA). Six serial dilutions of bovine serum albumin (BSA) were made in water (final concentration 0, 0.25, 0.5, 1, and 2 mg/mL). Four microliters of BSA were transferred to 96-well microtiter plate and diluted with 196 μL of the Bradford reagent to a final volume of 200 μL. Absorbance spectra were collected from 250 nm to 800 nm using a plate reader (Spark® 10M, catalog number: 30086376; Tecan, Männedorf, Switzerland). The assay was repeated as previously described with 4 μL of purified phiYFP and 196 μL of the Bradford reagent. The BSA absorbance values at 595 nm were plotted versus concentration (mg/mL) to generate a standard curve with a linear fit ($R^2 = 0.99$). To determine the extinction coefficient, purified phiYFP in 20 mM MOPS buffer (pH 7.5) was diluted to 5 μM 50 mM MES buffer (pH 5.5) in a 0.2-cm x 1-cm quartz cuvette (0.4 mL) (catalog number: 115F1040; Hellma USA, Plainview, NJ). Absorbance spectra were collected from 225 nm to 650 nm using the Agilent Cary 7000 Universal Measurement Spectrophotometer (catalog number: G687364000, Agilent, Santa Clara, CA). The Beer-Lambert law ($A=\varepsilon lc$) was used where the path length (l) is 1 cm and the concentration (c) is 5 μM. The extinction coefficient of phiYFP at pH 5.5 for the 525 nm absorbance peak in the absence and presence of 400 mM chloride is 86,531 ± 305 $M^{-1} \cdot cm^{-1}$ and 70,618 ± 305 $M^{-1} \cdot cm^{-1}$, respectively. The average of three technical replicates with standard error of the mean is reported.

SDS-PAGE and Coomassie Staining. Fifteen microliters of the purified protein was analyzed by sodium dodecyl sulfate polyacrylamide gel electrophoresis (SDS-PAGE) and diluted with 5 μL of 4X Laemmli sample buffer (catalog number: 1610747; Bio-Rad Laboratories, Hercules, CA) to a final volume of 20 μL (1X). The samples were boiled at 95 °C for 10 min, and then loaded onto a precast polyacrylamide gel (catalog number: 4561035; Bio-Rad Laboratories, Hercules, CA) along with 5 μL of the PageRuler™ Prestained Protein Ladder (catalog number: PI26616, Thermo Fisher Scientific, Waltham, MA). The loaded polyacrylamide gel was placed in a Mini-PROTEAN Tetra Cell (catalog number: 1645050; Bio-Rad Laboratories, Hercules, CA) containing 2.5 mM Tris, 19.2 mM glycine, and 0.01% SDS with an applied voltage of 200 mV for 20 min using a PowerPac™ power supply (catalog number: 1645050; Bio-Rad Laboratories, Hercules, CA). After electrophoresis, the gel was submerged in 0.025% Coomassie R250, 40% methanol, and 7% acetic acid staining solution, heated in a microwave for 30 s, and incubated

for 10 min at room temperature with orbital shaking. Then the staining solution was replaced with 75% DI water, 25% ethanol, and 5% acetic acid destaining solution and incubated for 15 min at room temperature with orbital shaking. This step was repeated four times with fresh destaining solution, and the gel incubated overnight with orbital shaking. The following day, the gel was washed with deionized water and analyzed (Figure S24).

General spectroscopic materials and methods. All spectroscopic measurements were carried out with a 0.2-cm x 1-cm quartz cuvette (0.4 mL) (catalog number: 115F1040; Hellma® USA, Plainview, NJ) unless stated otherwise. Absorbance spectra were collected on an Agilent Cary 7000 Universal Measurement Spectrophotometer equipped with a deuterium lamp source, a PbS detector, a two-colored Si/InGaAs detector, and a R928 photomultiplier tube (catalog number: G687364000 Agilent, Santa Clara, CA). Fluorescence spectra were collected on a Horiba Fluorolog®-3 equipped with a 450-W xenon short arc lamp source and power supply, a R928P photomultiplier tube, and two Spex® monochromator gratings (catalog number: 5500000439; Horiba, Kyoto, Japan).

Chloride titration and apparent dissociation constant determination for wild-type phiYFP and Q69 variants. Purified wild-type phiYFP and variants in 20 mM MOPS buffer (pH 7.5) were diluted 5-fold in 50 mM sodium citrate buffer (pH 5), 50 mM MES buffer (pH 5.5), or 50 mM MES (pH 6) and further diluted to ~5 μM with the corresponding buffer or buffer containing varying concentrations of sodium chloride. Absorbance spectra were collected from 250 nm to 650 nm. Excitation was provided at 525 nm, and the emission was collected from 530 nm to 650 nm (1-nm slit width). Variants were excited at 500 nm, and the emission was collected from 510 nm to 650 nm (1-nm slit width). All purified proteins were excited at 480 nm, and the emission was collected from 490 nm to 650 nm (1-nm slit width), and at 400 nm with emission collected from 405 nm to 650 nm (2-nm slit width). The emission was integrated from 405 nm to 650 nm with excitation provided at 400 nm and from 490 nm to 650 nm with excitation provided at 480 nm for all chloride concentrations using the *trapz* function in MATLAB R2017a and R2018a (MathWorks, Natwick, MA). The average of three technical replicates with the standard error of the mean is reported. The apparent dissociation constant (K_d) was determined by plotting the chloride concentration ($[Cl^-]$) versus the fractional binding [$F = (F_{obs} - F_{min})/(F_{max} - F_{min})$] in KaleidaGraph v4.5 (Synergy Software, Reading, PA) where F_{obs} is the integrated area of observed fluorescence intensity and F_{min} and F_{max} are the integrated area of fluorescence intensities at 0 mM and 400 mM sodium chloride, respectively. For the anions which have emission ratiometric response, the F_{obs} is the ratiometric emission response (λ_{em} = 540 nm / λ_{em} = 510 nm) with λ_{ex} = 400 nm, and F_{min} and F_{max} are the ratiometric emission response (λ_{em} = 540 nm / λ_{em} = 510 nm) with λ_{ex} = 400 nm at 0 mM and 400 mM sodium chloride, respectively. The apparent K_d was calculated using the following equation: $F = [Cl^-]/ (K_d + [Cl^-])$. The Hill coefficient was also determined by plotting log $[(F_{min}-F_{obs})/(F_{obs} -F_{max})]$ vs. log $[Cl^-]$ to a linear fit model (y = mx + b).[4] The average of three technical replicates with standard error of the mean is reported (Figure S5).

Chromophore pK_a determination for wild-type phiYFP and Q69 variants. To determine the chromophore pK_a in the absence and presence of 400 mM sodium chloride, 34 μL of purified protein in 20 mM MOPS buffer (pH 7.5) was diluted to ~5 μM in 50 mM sodium citrate buffer (pH 4, 4.5, and 5), 50 mM MES buffer (pH 5.5 and 6), 50 mM MOPS buffer (pH 6.5 and 7), 50 mM 4-(2-hydroxyethyl)-1-piperazineethanesulfonic acid (HEPES) buffer (pH 7.5 and 8), 50 mM bicine (pH 8.5), and 50 mM N-cyclohexyl-2-aminoethanesulfonic acid (CHES) buffer (pH 9) or 457 mM sodium chloride in the corresponding buffers. Absorbance spectra were collected from 250 nm to 650 nm. Excitation was provided at 525 nm, and the emission was collected from 530 nm to 650 nm (1-nm slit width). Variants were excited at 500 nm, and the emission was collected from 510 nm to 650 nm (1-nm slit width). All purified proteins were excited at 480 nm with the emission collected from 490 nm to 650 nm (1-nm slit width), and at 400 nm with the emission collected from 405 nm to 650 nm (2-nm slit width). The pH was plotted versus the average fluorescence response at 540 nm in KaleidaGraph and fitted to the Henderson-Hasselbach equation to determine the chromophore pK_a. The average of three technical replicates with standard error of the mean is reported.

Quantum yield determination for wild-type phiYFP. The quantum yield of wild-type phiYFP was determined in the presence and absence of 400 mM chloride. Six serial dilutions of purified phiYFP were prepared in 50 mM MES buffer (pH 5.5) or 50 mM MES buffer with 457 mM sodium chloride (pH 5.5). Absorbance spectra were collected from 250 nm to 650 nm. Six serial dilutions of coumarin 153 in ethanol (Φ = 0.54)[5] were used as a reference to determine the quantum yield of phiYFP when excited at 400 nm. Excitation was provided at 400 nm, and the emission was collected from 405 nm to 650 nm. The absorbance values for phiYFP at 400 nm and coumarin 153 at 425 nm were plotted versus the integrated emission from 405 nm to 650 nm to generate standard curves (R^2 > 0.99). Six serial dilutions of fluorescein in 100 mM sodium hydroxide (Φ = 0.92)[6] were used as a reference to determine the quantum yield of phiYFP when excited at 480 nm. Excitation was provided at 480 nm, and the emission was collected from 490 nm to 650 nm. The absorbance values for phiYFP at 525 nm and fluorescein at 490 nm were plotted versus the integrated emission from 490 nm to 650 nm to generate a standard curve (R^2 > 0.99). The absorption and fluorescence bandwidths were kept constant between samples. The wild-type phiYFP quantum yields in the presence and absence of 400 mM chloride were calculated using the equation: $\Phi_{YFP} = (slope_{YFP}/slope_{ref})(\eta_{YFP}^2/\eta_{ref}^2)$ where η are the refractive index values for water and ethanol.[7,8] The average of three technical replicates with standard error of the mean is reported (Figure S6).

Anion selectivity of wild-type phiYFP. Purified wild-type phiYFP in 20 mM MOPS buffer (pH 7.5) was diluted to 40 μM in 50 mM MES buffer (pH 5.5) and further diluted to ~5 μM 50 mM MES buffer containing varying concentrations of sodium bromide, sodium iodide, sodium nitrate, sodium phosphate, and sodium sulfate (pH 5.5). Absorbance spectra were collected from 250 nm to 650 nm. Excitation was provided at 525 nm with emission collected from 530 nm to 650 nm (1-nm slit width). Wild-type phiYFP was also excited at 480 nm with emission collected from 490 nm to 650 nm (1-nm slit width) and at 400 nm with emission collected from 405 nm to 650 nm (2-nm slit width). The emission was integrated from 405 nm to 650 nm with excitation provided at 400 nm and from 490 nm to 650 nm with excitation provided at 480 nm for salt all concentrations using the *trapz* function in MATLAB. Purified wild-type phiYFP in 20 mM MOPS buffer (pH 7.5) was diluted to 40 μM in 50 mM citrate buffer (pH 5) and 50mM MES buffer (pH 6) separately. The diluted protein was further diluted to ~5 μM in 50 mM citrate buffer (pH 5) or MES buffer (pH 6) containing varying concentrations of sodium bromide, sodium iodide, sodium nitrate, sodium phosphate, and sodium sulfate. Spectra for the anion selectivity at pH 5 and 6 were acquired on the Spark® 10M plate reader. Absorbance spectra were collected from 300 nm to 600 nm with 10-nm step size. Excitation was provided at 480 nm with emission collected from 500 nm to 600 nm with 10-nm step size, 40 flashes, and gain of 80 and at 400 nm with emission collected from 420 nm to 600 nm with 10-nm step size, 40 flashes, and gain of 100. The emission was integrated from 420 nm to 600 nm with excitation provided at 400 nm and from 500 nm to 600 nm with excitation provided at 480 nm for salt all concentrations using the *trapz* function in MATLAB. The apparent dissociation constant (K_d) for each anion was determined as described above, and the average of three technical replicates with the standard error of the mean is reported (Table S1).

Constant ionic strength with gluconate. Purified wild-type phiYFP in 20 mM MOPS buffer (pH 7.5) was diluted to 40 μM in 50 mM MES buffer (pH 5.5) and further diluted to ~5 μM in 50 mM MES buffer with 457 mM sodium gluconate (pH 5.5), 50 mM MES buffer with 228 mM sodium gluconate and 228 mM sodium chloride (pH 5.5), or 50 mM MES buffer with 457 mM sodium chloride (pH 5.5). Absorbance spectra were collected from 250 nm to 650 nm. Excitation was provided at 525 nm with emission collected from 530 nm to 650 nm (1-nm slit width), at 480 nm with emission collected from 490 nm to 650 nm (1-nm slit width), and at 400 nm with emission collected from 405 nm to 650 nm (2-nm slit width). The average of three technical replicates with the standard error of the mean is reported (Figure S7).

Chloride titration for avYFP-H148Q. Purified avYFP-H148Q in 20 mM MOPS buffer (pH 7.5) was diluted 5-fold in 50 mM sodium citrate buffer (pH 5), 50 mM MES buffer (pH 5.5), or 50 mM MES (pH 6) and further diluted to ~4 μM with 175 μL of the corresponding buffer or buffer containing varying concentrations of sodium chloride to a final volume of 200 μL. For each well, the absorbance spectra

were collected from 315 nm to 650 nm with 5-nm step size. Excitation was provided at 400 nm, and the emission was collected from 420 nm to 650 nm with 5-nm step size, 30 flashes, and gain of 150 on the Spark® 10M plate reader. Excitation was also provided at 480 nm, and the emission was collected from 495 nm to 650 nm with 5-nm step size, 30 flashes, and gain of 95. The average of three technical replicates with the standard error of the mean is reported (Figure S8).

Statistical Analysis. The average and sample standard deviation for all measurements was carried out using Microsoft Excel. The standard error of the mean was calculated by dividing the sample standard deviation by $\sqrt{n}$ where n is equal to the number of technical replicates. Two sample *t*-tests were used to determine significance by calculating the probability value (*p*-value).

```
Percent Identity  Matrix - created by Clustal2.1

    1: YFP-H148Q   100.00   51.29
    2: phiYFP       51.29  100.00
```

Figure S1. Percent identity matrix of avYFP-H148Q and phiYFP generated with Clustal Omega v2.1.[1]

```
CLUSTAL O(1.2.4) multiple sequence alignment

YFP-H148Q       MSKGEELFTGVVPILVELDGDVNGHKFSVSGEGEGDATYGKLTLKFICTTGKLPVPWPTL     60
phiYFP          MSSGALLFHGKIPYVVEMEGNVDGHTFSIRGKGYGDASVGKVDAQFICTTGDVPVPWSTL     60
                **.*  ** * :* :**:::*:*:**.**: *:* ***: **:  :******.:**** **

YFP-H148Q       VTTFGYGLQCFARYPDHMKQHDFFKSAMPEGYVQERTIFFKDDGNYKTRAEVKFEGDTLV     120
phiYFP          VTTLTYGAQCFAKYGPEL--KDFYKSCMPEGYVQERTITFEGDGVFKTRAEVTFENGSVY     118
                ***: ** ****:*  .:  :**:**.********** *:.** :******.**..::

YFP-H148Q       NRIELKGIDFKEDGNILGHKLEYNYNSQNVYIMADKQKNGIKVNFKIRHNIEDG--SVQL     178
phiYFP          NRVKLNGQGFKKDGHVLGKNLEFNFTPHCLYIWGDQANHGLKSAFKIMHEITGSKEDFIV     178
                **::*:* .**:**::**::**:*:. : :** .*: ::*:*  *** *:* ..  .. :

YFP-H148Q       ADHYQQNTPIGDGPVLLPDNHYLSYQSALSKDPNEKRDHMVLLEFVTAAGITHGMDELYK     238
phiYFP          ADHTQMNTPIGGGPVHVPEYHHITYHVTLSKDVTDHRDNMSLVETVRAVDCRKTYL----     234
                *** * *****.*** :*: *:::*: :**** .::**:* *:* * *..  :
```

Figure S2. Sequence alignment of avYFP-H148Q and phiYFP generated with Clustal Omega v1.2.4. [1] The residues that make up the chromophore are in blue, and the residues that are predicted to bind chloride are in red.

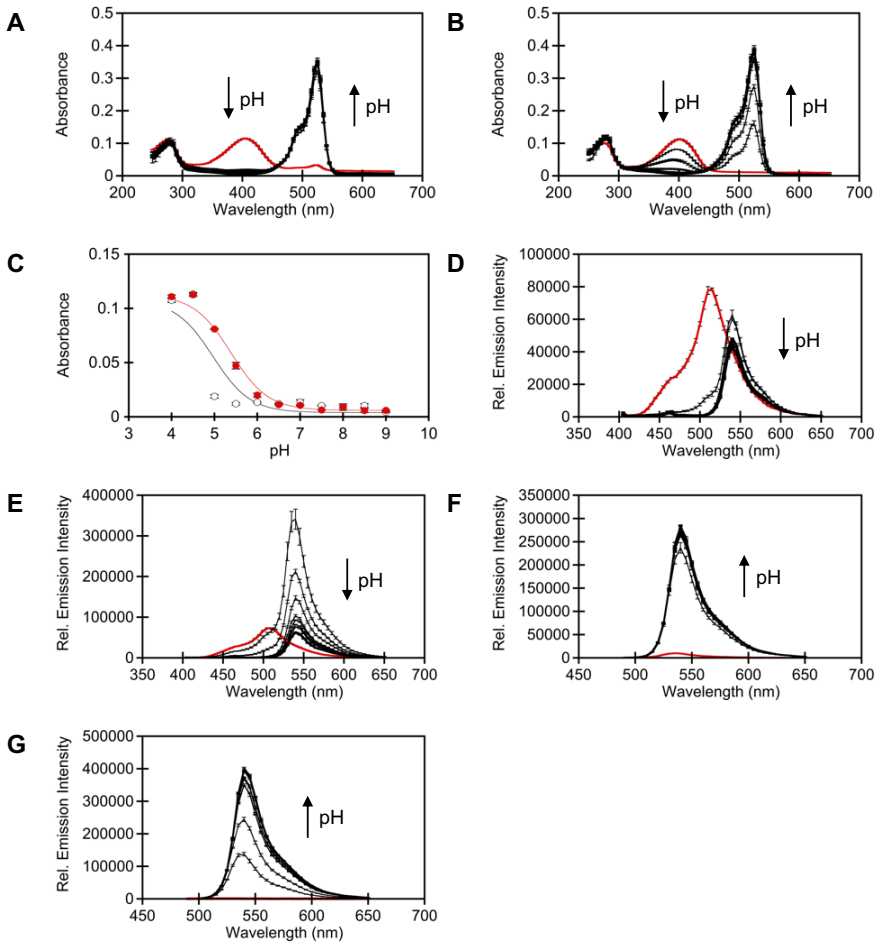

Figure S3. Spectroscopic properties of wild-type phiYFP as function of pH. UV-visible response of 5 μM phiYFP in the (A) absence and (B) presence of 400 mM chloride at pH 4.5 (red), 5, 5.5, 6, 6.5, 7, 7.5, 8, 8.5, and 9. (C) The absorbance values at 400 nm for the determination of the wild-type phiYFP chromophore pK_a in the presence (red circles) and absence (white circles) of 400 mM chloride. The pK_a in the absence and presence of chloride is 4.9 ± 0.02 and 5.4 ± 0.02, respectively. Emission response of 5 μM phiYFP in the (D) absence and (E) presence of chloride at pH 4.5 (red), 5, 5.5, 6, 6.5, 7, 7.5, 8, 8.5, and 9. Excitation was provided at 400 nm, and the emission was collected from 405 nm to 650 nm. Emission response of 5 μM phiYFP in the (F) absence and (G) presence of 400 mM chloride at pH 4.5 (red), 5, 5.5, 6, 6.5, 7, 7.5, 8, 8.5, and 9. Excitation was provided at 480 nm, and the emission was collected from 490 nm to 650 nm. All spectra were collected in 50 mM sodium citrate buffer (pH 4.5 and 5), 50 mM MES buffer (pH 5.5 and 6), 50 mM MOPS buffer (pH 6.5 and 7), 50 mM HEPES buffer (pH 7.5 and 8), 50 mM bicine (pH 8.5), and 50 mM CHES buffer (pH 9). Arrow direction corresponds to increasing pH. The average of three technical replicates with standard error of the mean is reported.

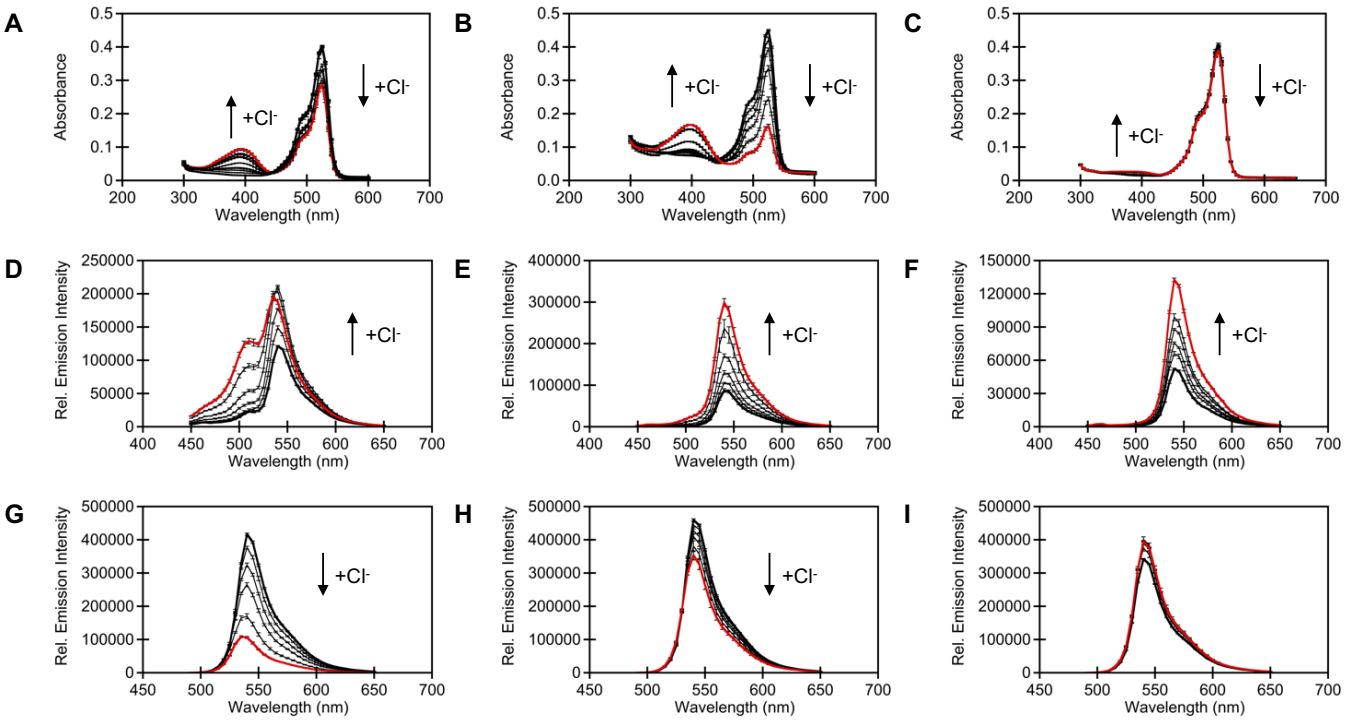

Figure S4. Spectroscopic characterization of wild-type phiYFP in the presence of chloride at varying pH. UV-visible response of 5 μM phiYFP at (A) pH 5, (B) pH 5.5, and (C) pH 6. Fluorescence response of 5 μM phiYFP. Excitation was provided at 400 nm, and the emission was collected from 405 nm to 650 nm at (D) pH 5, (E) pH 5.5, and (F) pH 6. Excitation was provided at 480 nm, and the emission was collected from 490 nm to 650 nm at (G) pH 5, (H) pH 5.5, and (I) pH 6. All spectra were acquired in 50 mM citrate buffer, pH 5, 50 mM MES buffer, pH 5.5, and 50 mM MES buffer, pH 6, in the presence of 0 (bold), 25, 50, 100, 200, and 400 mM chloride (red). Arrow direction corresponds to increasing chloride concentrations. The average of three technical replicates with standard error of the mean is reported.

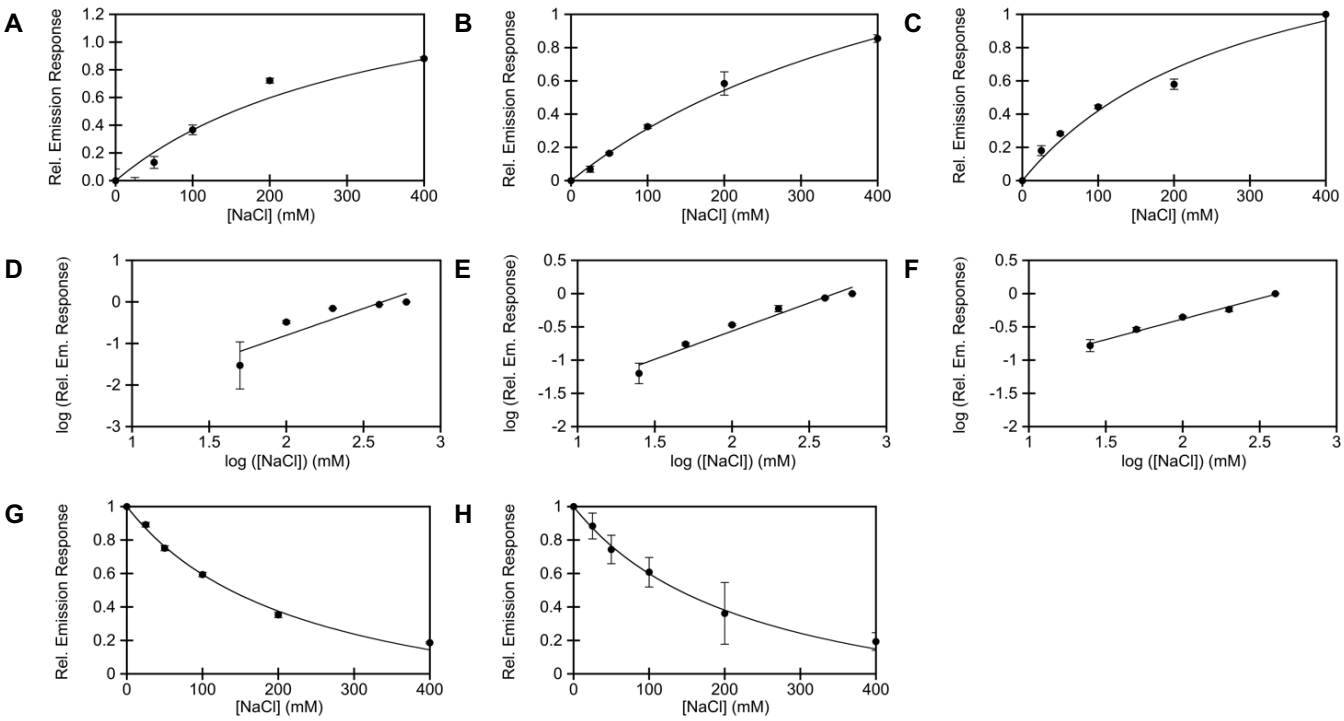

Figure S5. Fluorescence response of 5 μM wild-type phiYFP in the presence of 0, 25, 50, 100, 200, and 400 mM chloride at (A) pH 5, (B) pH 5.5, and (C) pH 6. Excitation was provided at 400 nm, and the emission was integrated from 405 nm to 650 nm. Hill plot of the fluorescence response of 5 μM phiYFP in presence of 25, 50, 100, 200, 400, and 600 mM chloride at (D) pH 5, (E) pH 5.5, and (F) pH 6. At pH 5, the apparent dissociation constant and Hill coefficient were determined using the ratiometric emission response (λ_{em} = 540 nm / λ_{em} = 510 nm). The Hill coefficients for pH 5, 5.5, and 6 are 0.79 ± 0.07, 0.90 ± 0.07, and 0.62 ± 0.06, respectively. Fluorescence response of 5 μM phiYFP in the presence of 0, 25, 50, 100, 200, and 400 mM chloride (G) at pH 5 and (H) pH 5.5. Excitation was provided at 480 nm, and the emission was integrated from 490 nm to 650 nm. All spectra were acquired in 50 mM citrate buffer, pH 5, 50 mM MES buffer, pH 5.5, and 50 mM MES buffer, pH 6. The average of three technical replicates with standard error of the mean is reported.

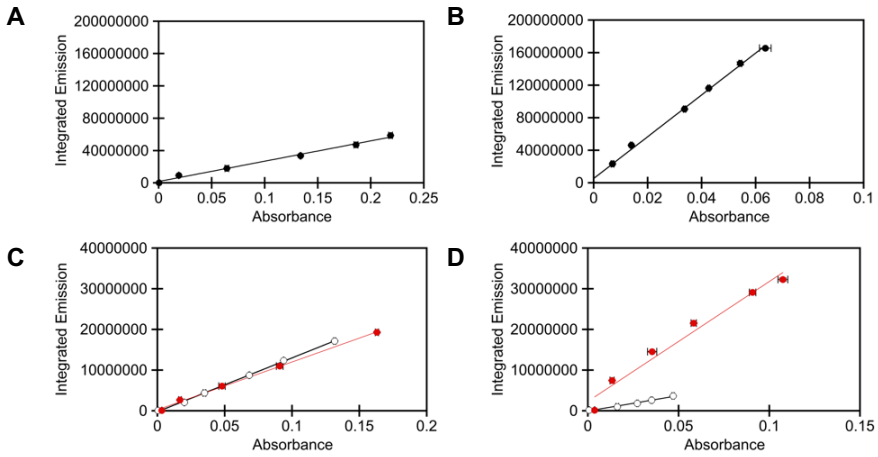

Figure S6. (A) Quantum yield standard curve for fluorescein in 100 mM NaOH. Absorbance values at 490 nm were plotted versus the emission response ($R^2 > 0.99$). Excitation was provided at 480 nm, and the emission was integrated from 490 nm to 650 nm. (B) Quantum yield standard curve for coumarin 153 in ethanol. Absorbance values at 425 nm were plotted versus the emission response ($R^2 > 0.99$). Excitation was provided at 400 nm, and the emission was integrated from 405 nm to 750 nm. (C) Quantum yield standard curve for wild-type phiYFP in the absence (white circles) and presence (red circles) of 400 mM chloride. Absorbance values at 480 nm were plotted versus the emission response ($R^2 > 0.99$). Excitation was provided at 480 nm, and the emission was integrated from 490 nm to 650 nm. The phiYFP quantum yield is $\Phi = 0.49 \pm 0.002$ and $\Phi = 0.44 \pm 0.002$ in the absence and presence of 400 mM chloride, respectively. (D) Quantum yield standard curve for wild-type phiYFP in the absence (white circles) and presence (red circles) of 400 mM chloride. Absorbance values at 400 nm were plotted versus the emission response ($R^2 > 0.99$). Excitation was provided at 400 nm, and the emission was integrated from 405 nm to 650 nm. The phiYFP quantum yield is $\Phi = 0.02 \pm 0.002$ and $\Phi = 0.06 \pm 0.001$ in the absence and presence of 400 mM chloride, respectively. Spectra were collected in 50 mM MES buffer, pH 5.5 or 50 mM MES buffer with 400 mM chloride, pH 5.5. The average of three technical replicates with standard error of the mean is reported.

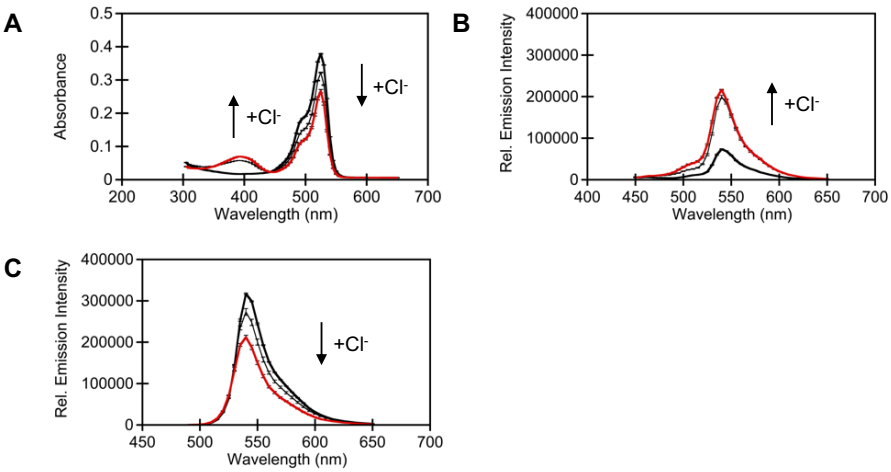

Figure S7. Spectroscopic characterization of wild-type phiYFP at pH 5.5 under constant ionic strength with gluconate. (A) UV-visible response of 5 μM phiYFP to chloride. Emission response of 5 μM phiYFP to chloride. (B) Excitation was provided at 400 nm, and the emission was collected from 405 nm to 650 nm. (C) Excitation was provided at 480 nm, and the emission was collected from 490 nm to 650 nm. All spectra were acquired in 50 mM MES buffer, pH 5.5 in the presence of 0 mM chloride/400 mM gluconate (bold), 200 mM chloride/200 mM gluconate, or 400 mM chloride/0 mM gluconate (red). Arrow direction corresponds to increasing chloride concentrations. The average of three technical replicates with standard error of the mean is reported.

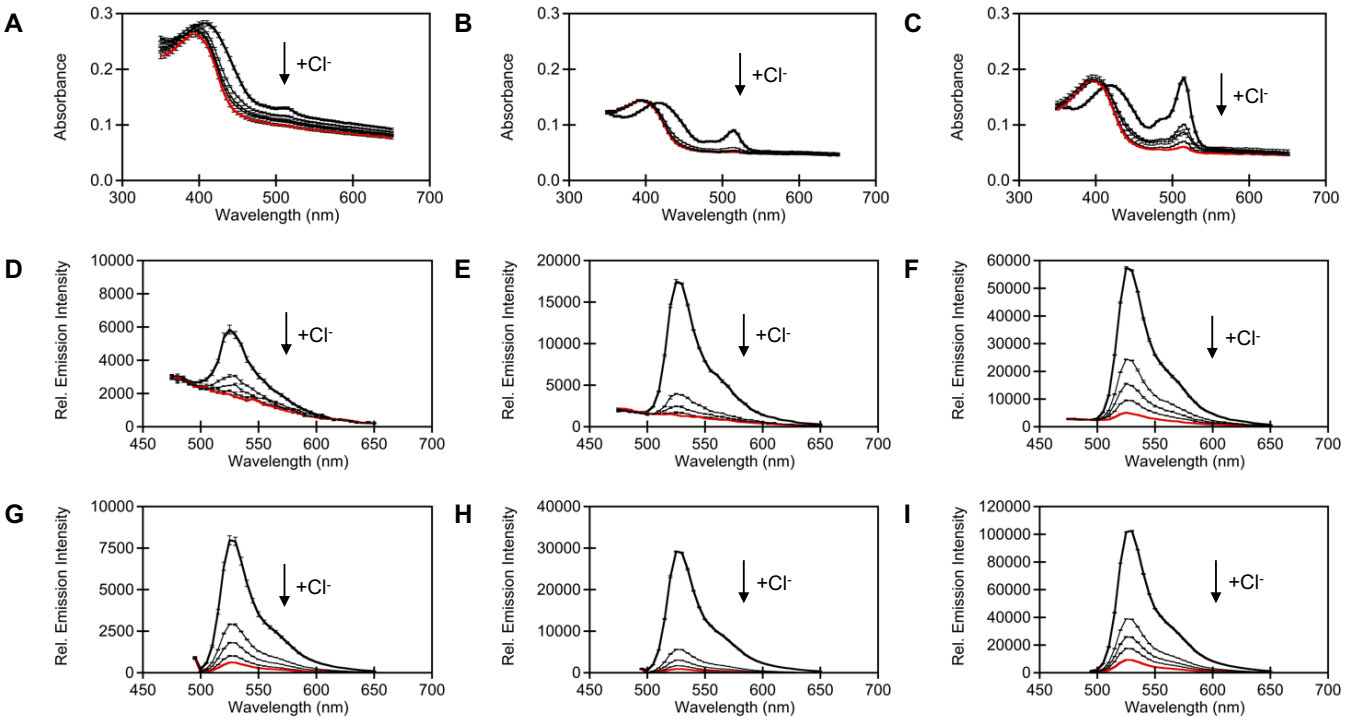

Figure S8. Spectroscopic characterization of avYFP-H148Q in the presence of chloride at varying pH. UV-visible response of 4 μM avYFP-H148Q at (A) pH 5, (B) pH 5.5, and (C) pH 6. Fluorescence response of 4 μM avYFP-H148Q to 0 (bold), 50, 100, 200, and 400 mM chloride (red). Excitation was provided at 400 nm, and the emission was collected from 420 nm to 650 nm at (D) pH 5, (E) pH 5.5, and (F) pH 6. Excitation was provided at 480 nm, and the emission was collected from 490 nm to 650 nm at (G) pH 5, (H) pH 5.5, and (I) pH 6. All spectra were acquired in 50 mM citrate buffer, pH 5, 50 mM MES buffer, pH 5.5, and 50 mM MES buffer, pH 6. Arrow direction corresponds to increasing chloride concentrations. The average of three technical replicates with standard error of the mean is reported.

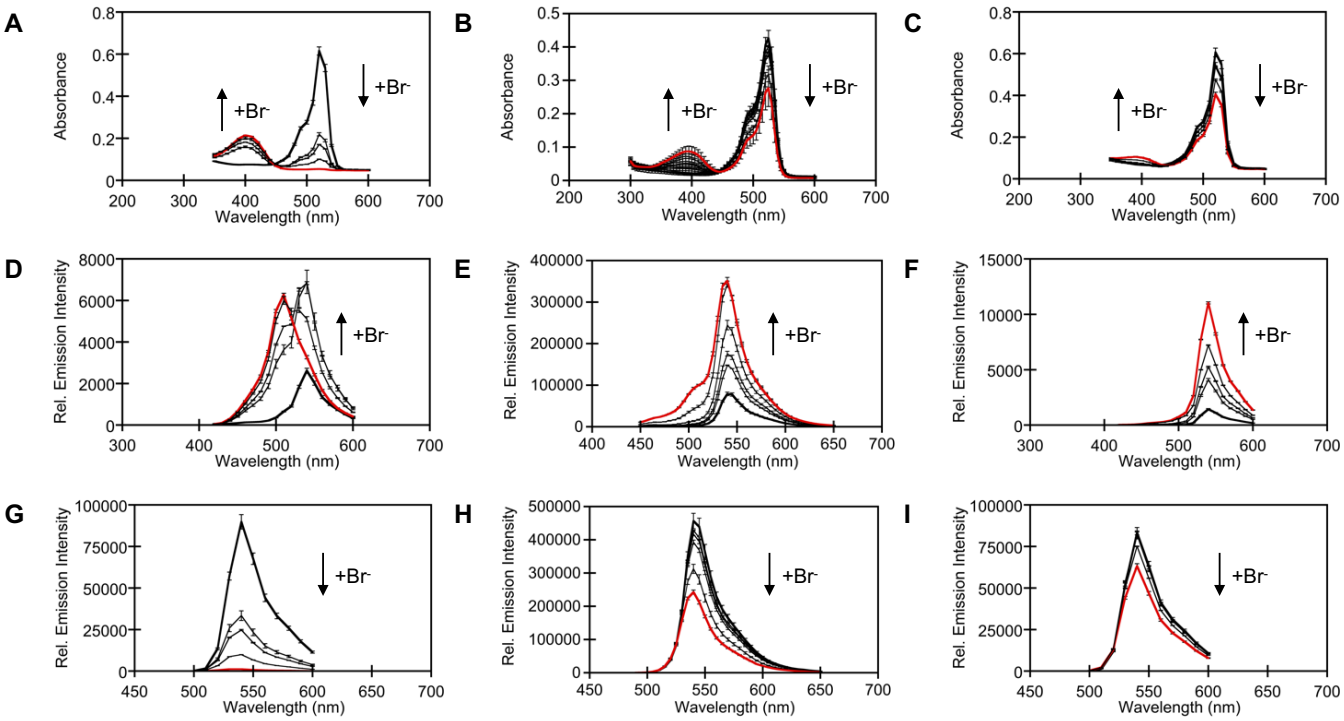

Figure S9. Spectroscopic characterization of wild-type phiYFP in the presence of bromide at varying pH. UV-visible response of 5 μM phiYFP at (A) pH 5, (B) pH 5.5, and (C) pH 6. Fluorescence response of 5 μM phiYFP. Excitation was provided at 400 nm, and the emission was collected from 420 nm to 600 nm at (D) pH 5, (E) pH 5.5, and (F) pH 6. Excitation was provided at 480 nm, and the emission was collected from 500 nm to 600 nm at (G) pH 5, (H) pH 5.5, and (I) pH 6. All spectra were acquired in 50 mM citrate buffer, pH 5, 50 mM MES buffer, pH 5.5, and 50 mM MES buffer, pH 6, in the presence of 0 (bold), 25, 50, 100, 200, and 400 mM bromide (red). Arrow direction corresponds to increasing bromide concentrations. The average of three technical replicates with standard error of the mean is reported.

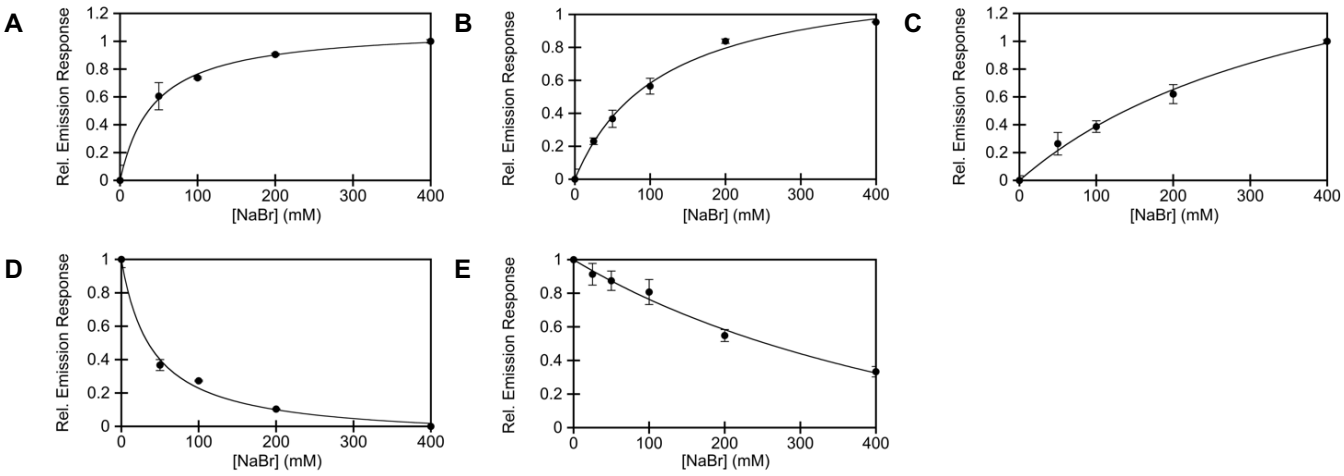

Figure S10. Fluorescence response of 5 µM wild-type phiYFP in the presence of 0, 25, 50, 100, 200, and 400 mM bromide (A) at pH 5, (B) pH 5.5, and (C) pH 6. Excitation was provided at 400 nm, and the emission was integrated from 405 nm to 650 nm. At pH 5 and 5.5, the apparent dissociation constant was determined using the ratiometric emission response (λ_{em} = 540 nm / λ_{em} = 510 nm). Fluorescence response of 5 µM phiYFP in the presence of 0, 25, 50, 100, 200, and 400 mM bromide (D) at pH 5 and (E) pH 5.5. Excitation was provided at 480 nm, and the emission was integrated from 490 nm to 650 nm. All spectra were acquired in 50 mM citrate buffer, pH 5, 50 mM MES buffer, pH 5.5, and 50 mM MES buffer, pH 6. The average of three technical replicates with standard error of the mean is reported.

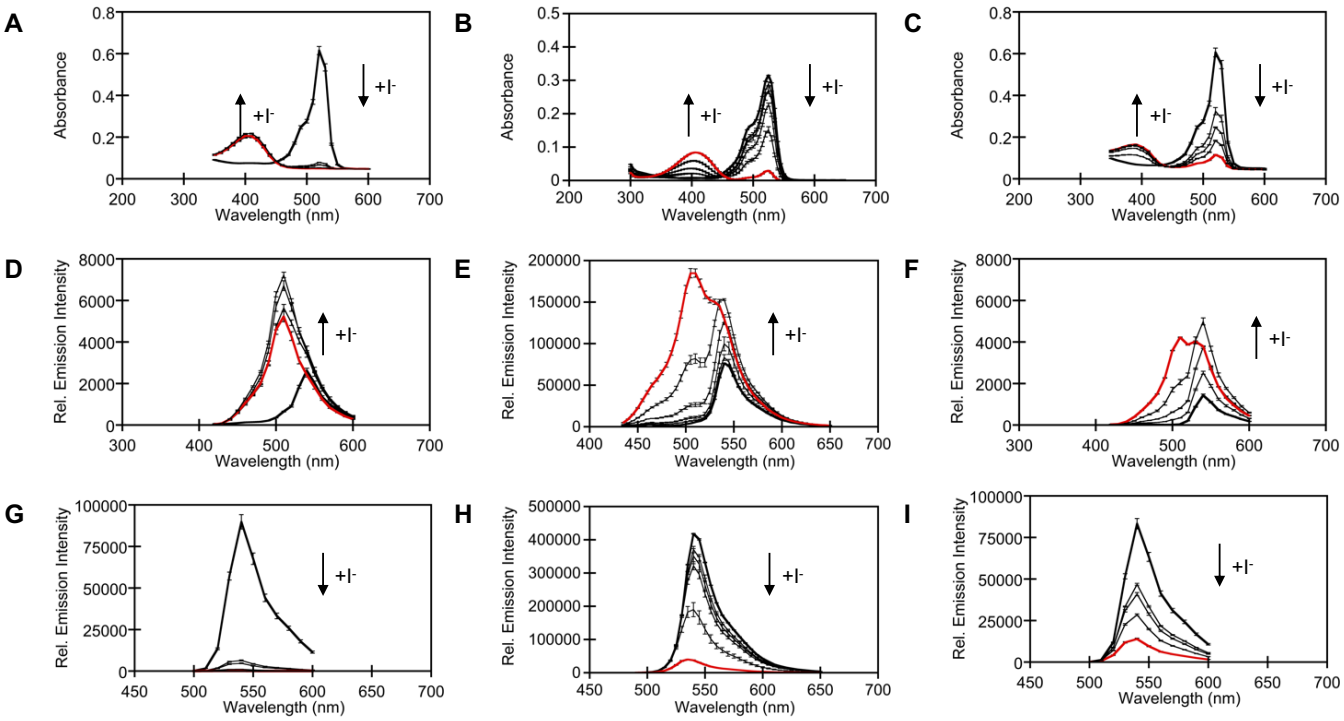

Figure S11. Spectroscopic characterization of wild-type phiYFP in the presence of iodide at varying pH. UV-visible response of 5 μM phiYFP at (A) pH 5, (B) pH 5.5, and (C) pH 6. Fluorescence response of 5 μM phiYFP. Excitation was provided at 400 nm, and the emission was collected from 420 nm to 600 nm at (D) pH 5, (E) pH 5.5, and (F) pH 6. Excitation was provided at 480 nm, and the emission was collected from 500 nm to 600 nm at (G) pH 5, (H) pH 5.5, and (I) pH 6. All spectra were acquired in 50 mM citrate buffer, pH 5, 50 mM MES buffer, pH 5.5, and 50 mM MES buffer, pH 6, in the presence of 0 (bold), 25, 50, 100, 200, and 400 mM iodide (red). Arrow direction corresponds to increasing iodide concentrations. The average of three technical replicates with standard error of the mean is reported.

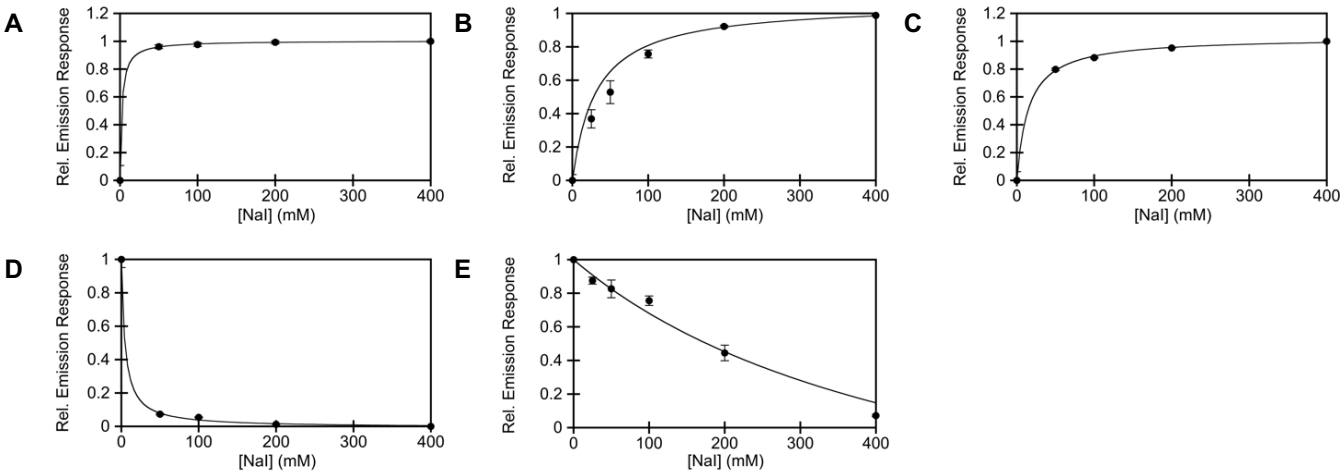

Figure S12. Fluorescence response of 5 µM wild-type phiYFP in the presence of 0, 25, 50, 100, 200, and 400 mM iodide (A) at pH 5, (B) pH 5.5, and (C) pH 6. Excitation was provided at 400 nm, and the emission was collected from 405 nm to 650 nm. The apparent dissociation constants at pH 5, 5.5, and 6 were determined using the ratiometric emission response (λ_{em} = 540 nm / λ_{em} = 510 nm). Fluorescence response of 5 µM phiYFP in the presence of 0, 25, 50, 100, 200, and 400 mM iodide (D) at pH 5 and (E) pH 5.5. Excitation was provided at 480 nm, and the emission was integrated from 490 nm to 650 nm. All spectra were acquired in 50 mM citrate buffer, pH 5, 50 mM MES buffer, pH 5.5, and 50 mM MES buffer, pH 6. The average of three technical replicates with standard error of the mean is reported.

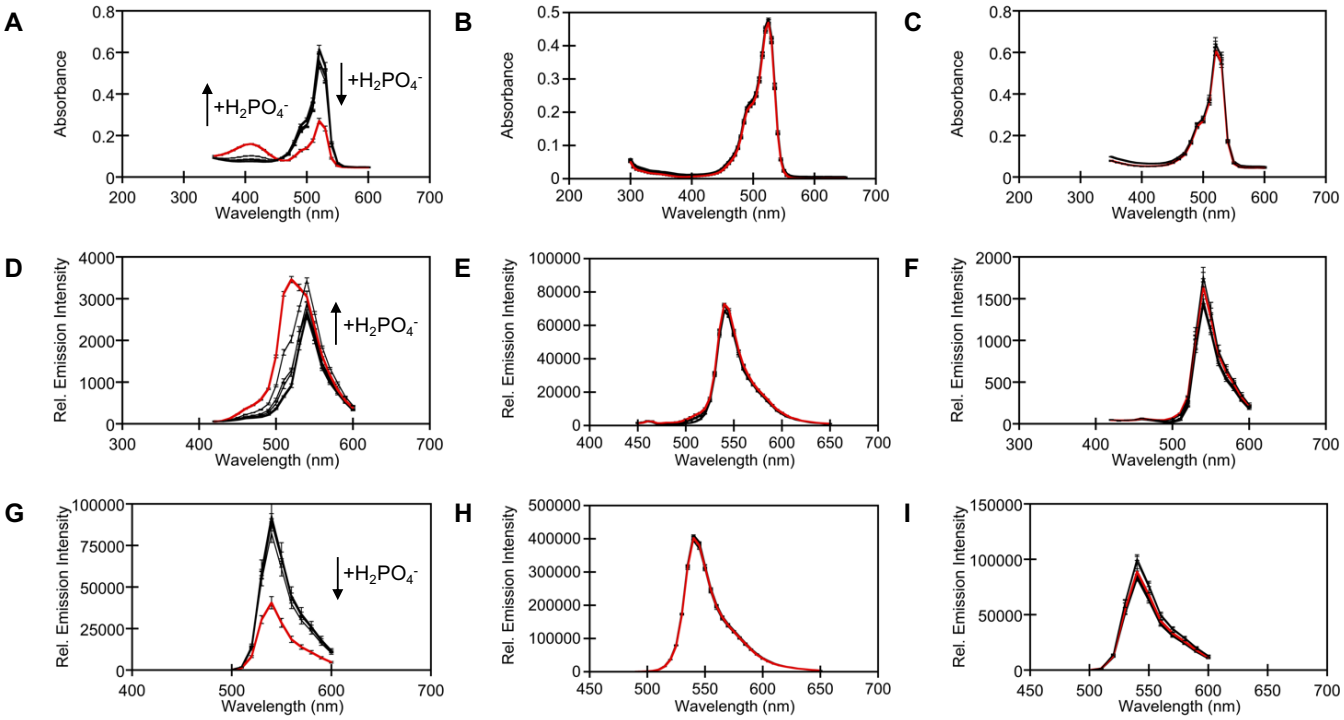

Figure S13. Spectroscopic characterization of wild-type phiYFP in the presence of dihydrogen phosphate at varying pH. UV-visible response of 5 μM phiYFP at (A) pH 5, (B) pH 5.5, and (C) pH 6. Fluorescence response of 5 μM phiYFP. Excitation was provided at 400 nm, and the emission was collected from 420 nm to 600 nm at (D) pH 5, (E) pH 5.5, and (F) pH 6. Excitation was provided at 480 nm, and the emission was collected from 500 nm to 600 nm at (G) pH 5, (H) pH 5.5, and (I) pH 6. All spectra were acquired in 50 mM citrate buffer, pH 5, 50 mM MES buffer, pH 5.5, and 50 mM MES buffer, pH 6, in the presence of 0 (bold), 25, 50, 100, 200, and 400 mM dihydrogen phosphate (red). Arrow direction corresponds to increasing dihydrogen phosphate concentrations. The average of three technical replicates with standard error of the mean is reported.

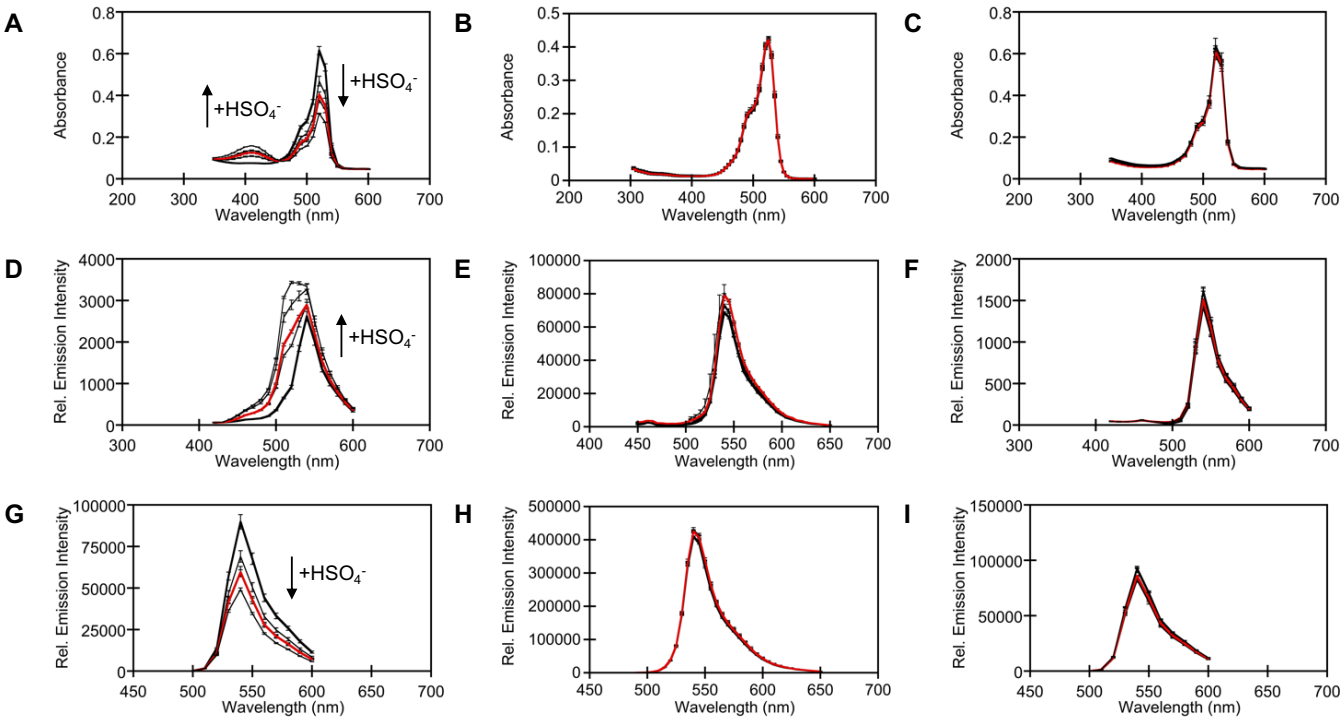

Figure S14. Spectroscopic characterization of wild-type phiYFP in the presence of hydrogen sulfate at varying pH. UV-visible response of 5 μM phiYFP at (A) pH 5, (B) pH 5.5, and (C) pH 6. Fluorescence response of 5 μM phiYFP. Excitation was provided at 400 nm, and the emission was collected from 420 nm to 600 nm at (D) pH 5, (E) pH 5.5, and (F) pH 6. Excitation was provided at 480 nm, and the emission was collected from 500 nm to 600 nm at (G) pH 5, (H) pH 5.5, and (I) pH 6. All spectra were acquired in 50 mM citrate buffer, pH 5, 50 mM MES buffer, pH 5.5, and 50 mM MES buffer, pH 6, in the presence of 0 (bold), 25, 50, 100, 200, and 400 mM hydrogen sulfate (red). Arrow direction corresponds to increasing hydrogen sulfate concentrations. The average of three technical replicates with standard error of the mean is reported.

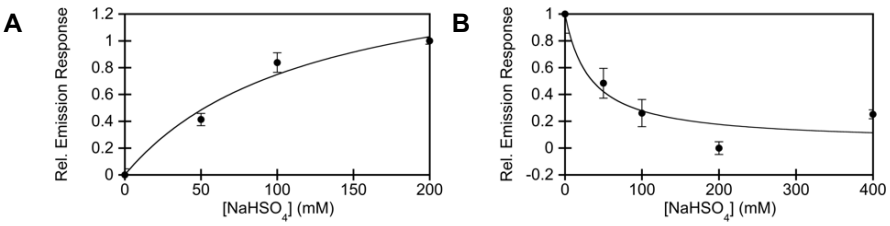

Figure S15. Fluorescence response of 5 μM wild-type phiYFP in the presence of 0, 25, 50, 100, 200, and 400 mM hydrogen sulfate at pH 5. (A) Excitation was provided at 400 nm, and the emission was integrated from 420 nm to 600 nm. (B) Excitation was provided at 480 nm, and the emission was integrated from 490 nm to 650 nm. All spectra were acquired in 50 mM citrate buffer, pH 5. The average of three technical replicates with standard error of the mean is reported.

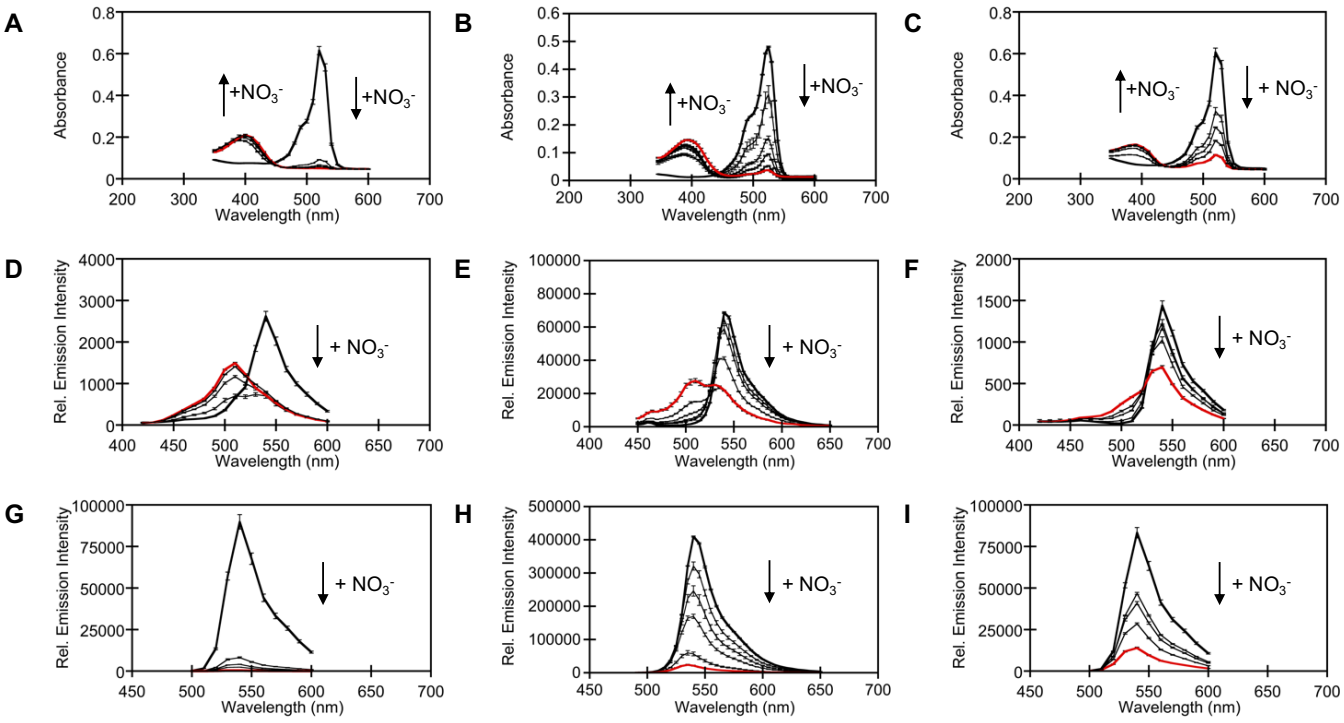

Figure S16. Spectroscopic characterization of wild-type phiYFP in the presence of nitrate at varying pH. UV-visible response of 5 μM phiYFP at (A) pH 5, (B) pH 5.5, and (C) pH 6. Fluorescence response of 5 μM phiYFP. Excitation was provided at 400 nm, and the emission was collected from 420 nm to 600 nm at (D) pH 5, (E) pH 5.5, and (F) pH 6. Excitation was provided at 480 nm, and the emission was collected from 500 nm to 600 nm at (G) pH 5, (H) pH 5.5, and (I) pH 6. All spectra were acquired in 50 mM citrate buffer, pH 5, 50 mM MES buffer, pH 5.5, and 50 mM MES buffer, pH 6, in the presence of 0 (bold), 25, 50, 100, 200, and 400 mM nitrate (red). Arrow direction corresponds to increasing nitrate concentrations. The average of three technical replicates with standard error of the mean is reported.

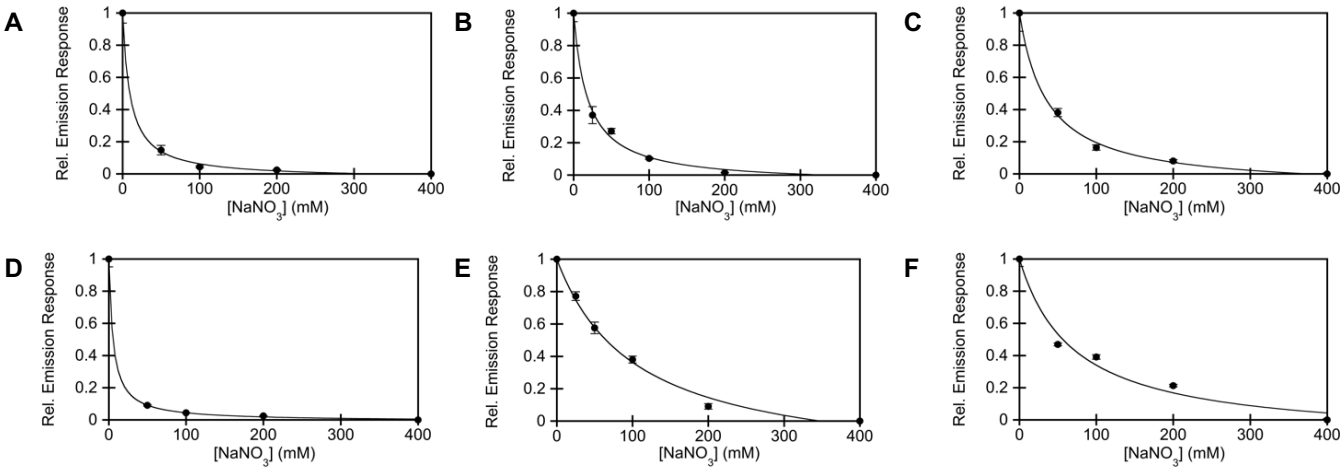

Figure S17. Fluorescence response of 5 μM wild-type phiYFP in the presence of 0, 25, 50, 100, 200, and 400 mM nitrate (A) at pH 5, (B) pH 5.5, and (C) pH 6. Excitation was provided at 400 nm, and the emission was collected from 405 nm to 650 nm. The apparent dissociation constants at pH 5, 5.5, and 6 determined using the ratiometric emission response (λ_{em} = 540 nm / λ_{em} = 510 nm). Fluorescence response of 5 μM wild-type phiYFP in the presence of nitrate (D) at pH 5, (E) pH 5.5, and (F) pH 6. Excitation was provided at 480 nm, and the emission was integrated from 490 nm to 650 nm. All spectra were acquired in 50 mM citrate buffer, pH 5, 50 mM MES buffer, pH 5.5, and 50 mM MES buffer, pH 6. The average of three technical replicates with standard error of the mean is reported.

Table S1. Summary of the phiYFP (5 μM) emission response to chloride and other anions as a function of pH. Spectra were collected in 50 mM sodium citrate buffer, pH 5, and 50 mM MES buffer, pH 5.5 and pH 6. The sodium salt was used for all of the anions tested.

Anion	pH	λ_{ex} = 400 nm [b]		λ_{ex} = 480 nm [b]		R / R_0 ± S.E.M. [c]
		F_f / F_0 ± S.E.M.	K_d (mM) ± S.E.M.	F_f / F_0 ± S.E.M.	K_d (mM) ± S.E.M.	
Cl^-	5	2.3 ± 0.1	290 ± 44 [d]	0.27 ± 0.01	239 ± 26	8.6 ± 0.3
	5.5	3.5 ± 0.1	384 ± 46	0.77 ± 0.04	322 ± 161	4.5 ± 0.2
	6	2.5 ± 0.02	306 ± 38	1.1 ± 0.09	ND	2.2 ± 0.02
Br^-	5	3.6 ± 0.3 [a]	44 ± 4 [d]	0.016 ± 0.002	40 ± 7	198 ± 11
	5.5	5.4 ± 0.3	106 ± 5 [d]	0.53 ± 0.02	608 ± 209	10 ± 0.5
	6	8.0 ± 0.5	417 ± 100	0.78 ± 0.05	ND	10 ± 0.02
I^-	5	3.5 ± 0.3 [a]	2.3 ± 0.2 [d]	0.0025 ± 0.0002	4.7 ± 0.9	1033 ± 35
	5.5	4.2 ± 0.1	50 ± 2 [d]	0.10 ± 0.003	577 ± 153	43 ± 2
	6	5.5 ± 0.5	15 ± 1 [d]	0.33 ± 0.040	ND	16 ± 1
$H_2PO_4^-$	5	1.8 ± 0.2	ND	0.45 ± 0.04	ND	4.0 ± 0.12
	5.5	1.1 ± 0.02	ND	1.0 ± 0.01	ND	1.1 ± 0.01
	6	1.2 ± 0.2	ND	ND	ND	1.1 ± 0.1
HSO_4^-	5	1.9 ± 0.2 [a]	121 ± 63	0.66 ± 0.05	33 ± 27	2.2 ± 0.05
	5.5	1.2 ± 0.01	ND	1.0 ± 0.01	ND	1.2 ± 0.01
	6	1.2 ± 0.07 [a]	ND	ND	ND	1.0 ± 0.02
NO_3^-	5	ND	9.8 ± 1 [d]	0.0043 ± 0.0004	5.5 ± 0.4	180 ± 5
	5.5	0.81 ± 0.02	19 ± 4 [d]	0.06 ± 0.01	103 ± 7	14 ± 1
	6	0.27 ± 0.07	36 ± 4 [d]	0.18 ± 0.02	71 ± 20	4.1 ± 0.2

[a] *Determined with 200 mM anion because fluorescence quenching was observed with higher salt concentrations*
[b] *Determined with 400 mM chloride*
[c] *Ratiometric response of apo phiYFP (R_0) to anion where* $R = F_{ex = 400\ nm} / F_{ex = 480\ nm}$
[d] *Emission ratiometric response (*λ_{em} = 540 nm / λ_{em} = 510 nm).

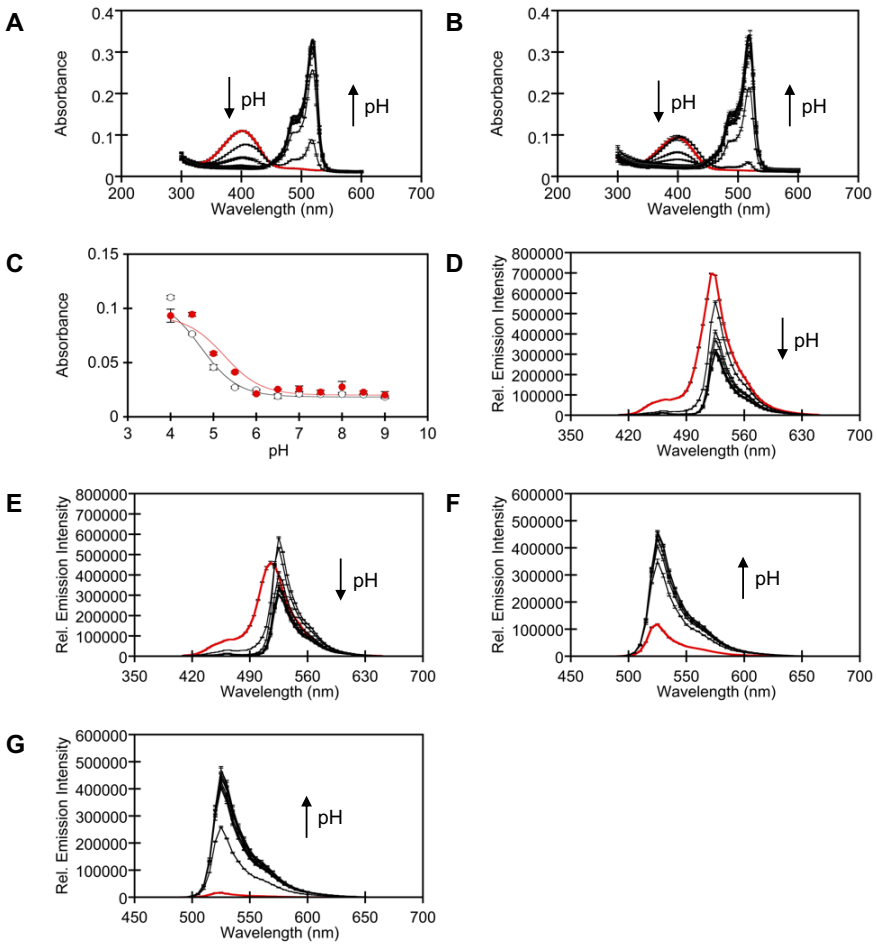

Figure S18. Spectroscopic properties of phiYFP Q69L as function of pH. UV-visible response of 4.4 µM phiYFP Q69L in the (A) absence and (B) presence of 400 mM chloride at pH 4.5 (red), 5, 5.5, 6, 6.5, 7, 7.5, 8, 8.5, and 9. (C) Determination of the phiYFP Q69L chromophore pK_a in the presence (red circles) and absence (white circles) of 400 mM chloride. UV-visible response of 4.4 µM phiYFP Q69L at 400 nm. The phiYFP Q69L pK_a in the absence and presence of chloride is 4.7 ± 0.8 and 5.2 ± 0.01, respectively. Emission response of 4.4 µM phiYFP Q69L in the (D) absence and (E) presence of 400 mM chloride at pH 4.5 (red), 5, 5.5, 6, 6.5, 7, 7.5, 8, 8.5, and 9. Excitation was provided at 400 nm, and the emission was collected from 405 nm to 650 nm. Emission response of 4.4 µM phiYFP Q69L in the (F) absence and (G) presence of 400 mM chloride at pH 4.5 (red), 5, 5.5, 6, 6.5, 7, 7.5, 8, 8.5, and 9. Excitation was provided at 480 nm, and the emission was collected from 490 nm to 650 nm. All spectra were collected in 50 mM sodium citrate buffer (pH 4.5 and 5), 50 mM MES buffer (pH 5.5 and 6), 50 mM MOPS buffer (pH 6.5 and 7), 50 mM HEPES buffer (pH 7.5 and 8), 50 mM bicine (pH 8.5), and 50 mM CHES buffer (pH 9). Arrow direction corresponds to increasing pH. The average of three technical replicates with standard error of the mean is reported.

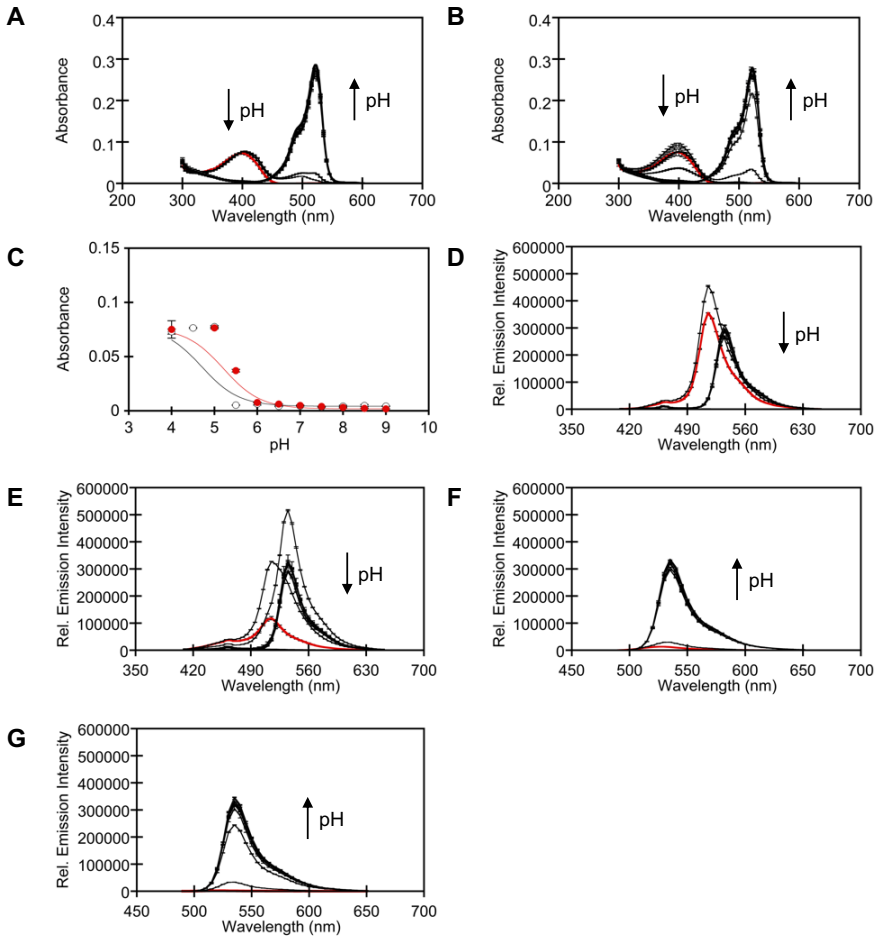

Figure S19. Spectroscopic properties of phiYFP Q69H as a function of pH. UV-visible response of 4.4 μM phiYFP Q69H in the (A) absence and (B) presence of 400 mM chloride at pH 4.5 (red), 5, 5.5, 6, 6.5, 7, 7.5, 8, 8.5, and 9. (C) Determination of the phiYFP Q69H chromophore pK_a in the presence (red circles) and absence (white circles) of 400 mM chloride. UV-visible response of 4.4 μM phiYFP at 400 nm. The phiYFP Q69H pK_a in the absence and presence of chloride is 4.7 ± 0.007 and 5.2 ± 0.008, respectively. Emission response of 4.4 μM phiYFP Q69H in the (D) absence and (E) presence of 400 mM chloride at pH 4.5 (red), 5, 5.5, 6, 6.5, 7, 7.5, 8, 8.5, and 9. Excitation was provided at 400 nm, and the emission was collected from 405 nm to 650 nm. Emission response of 4.4 μM phiYFP Q69H in the (F) absence and (G) presence of 400 mM chloride at pH 4.5 (red), 5, 5.5, 6, 6.5, 7, 7.5, 8, 8.5, and 9. Excitation was provided at 480 nm, and the emission was collected from 490 nm to 650 nm. All spectra were collected in 50 mM sodium citrate buffer (pH 4.5 and 5), 50 mM MES buffer (pH 5.5 and 6), 50 mM MOPS buffer (pH 6.5 and 7), 50 mM HEPES buffer (pH 7.5 and 8), 50 mM bicine (pH 8.5), and 50 mM CHES buffer (pH 9). Arrow direction corresponds to increasing pH. The average of three technical replicates with standard error of the mean is reported.

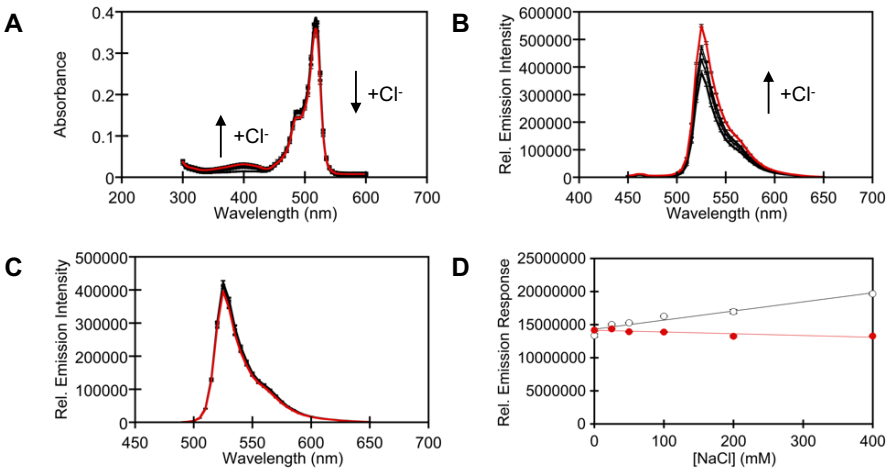

Figure S20. Spectroscopic characterization of phiYFP Q69L in the presence of chloride at pH 5.5. (A) UV-visible response of 4.4 µM phiYFP Q69L. Emission response of 4.4 µM phiYFP. (B) Excitation was provided at 400 nm, and the emission was collected from 450 nm to 650 nm. (C) Excitation was provided at 480 nm, and the emission was collected from 490 nm to 650 nm. All spectra were acquired in 50 mM MES buffer, pH 5.5 in the presence of 0, 25, 50, 100, 200, and 400 mM chloride (red). Arrow direction corresponds to increasing chloride concentrations. (D) Emission response from 4.4 µM phiYFP Q69L in the presence of 0, 25, 50, 100, 200, and 400 mM chloride. Excitation was provided at 400 nm, and the emission was integrated from 450 nm to 650 nm (white circles). Excitation was provided at 480 nm, and the emission was integrated from 490 nm to 650 nm (red circles). The average of three technical replicates with standard error of the mean is reported.

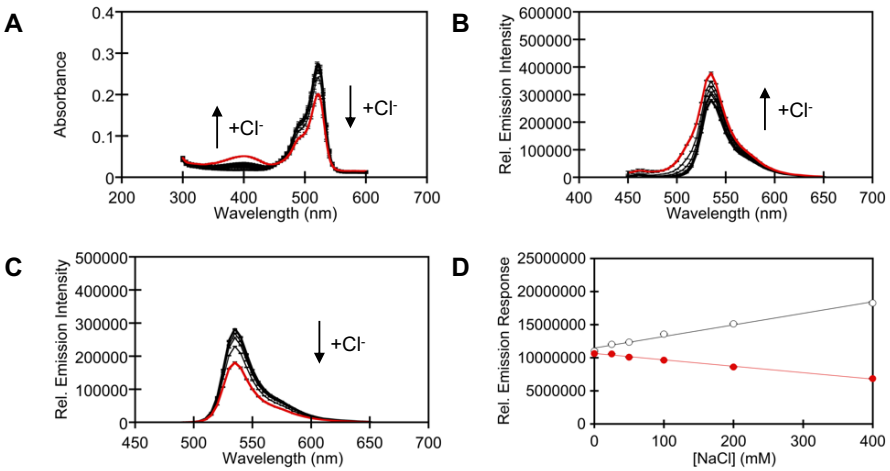

Figure S21. Spectroscopic characterization of phiYFP Q69H in the presence of chloride at pH 5.5. (A) UV-visible response of 4.4 µM phiYFP Q69H. Emission response of 4.4 µM phiYFP. (B) Excitation was provided at 400 nm, and the emission was collected from 450 nm to 650 nm. (C) Excitation was provided at 480 nm, and the emission was collected from 490 nm to 650 nm. All spectra were acquired in 50 mM MES buffer, pH 5.5 in the presence of 0, 25, 50, 100, 200, and 400 mM chloride (red). Arrow direction corresponds to increasing chloride concentrations. (D) Emission response from 4.4 µM phiYFP Q69H in the presence of 0, 25, 50, 100, 200, and 400 mM chloride. Excitation was provided at 400 nm, and the emission was integrated from 450 nm to 650 nm (white circles). Excitation was provided at 480 nm, and the emission was integrated from 490 nm to 650 nm (red circles). The average of three technical replicates with standard error of the mean is reported.

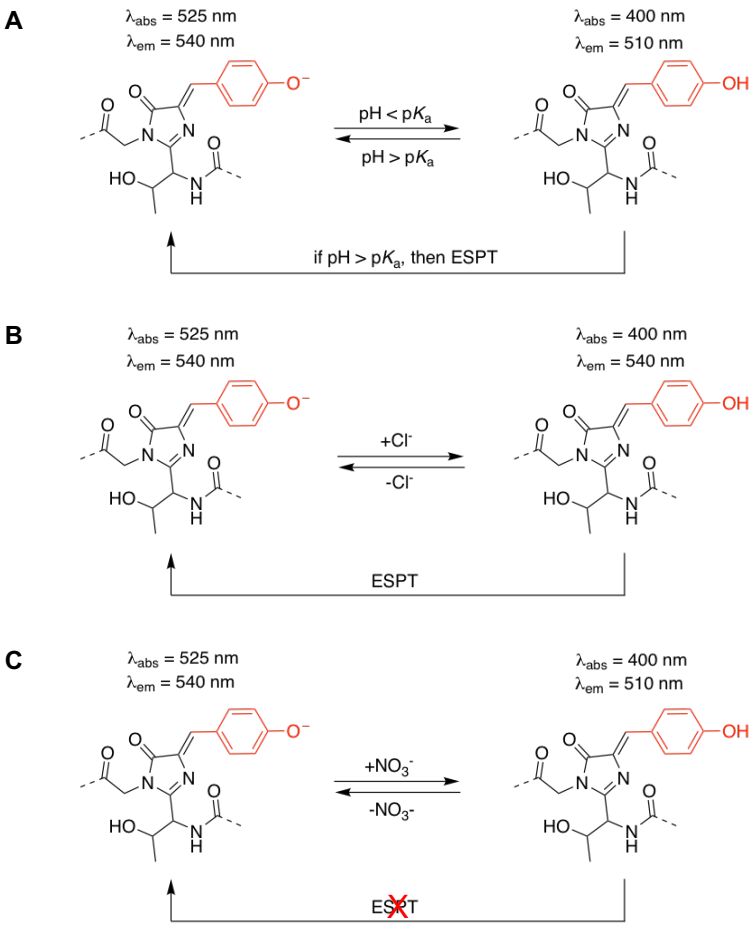

Figure S22. (A) Proposed model for the emission response of wild-type phiYFP as a function of pH (Figure S3). (B) Proposed model for wild-type phiYFP turn-on fluorescence response with chloride at pH 5.5 (Figure S4). (C) Proposed model for wild-type phiYFP turn-off fluorescence response with nitrate at pH 5.5 (Figure S16).

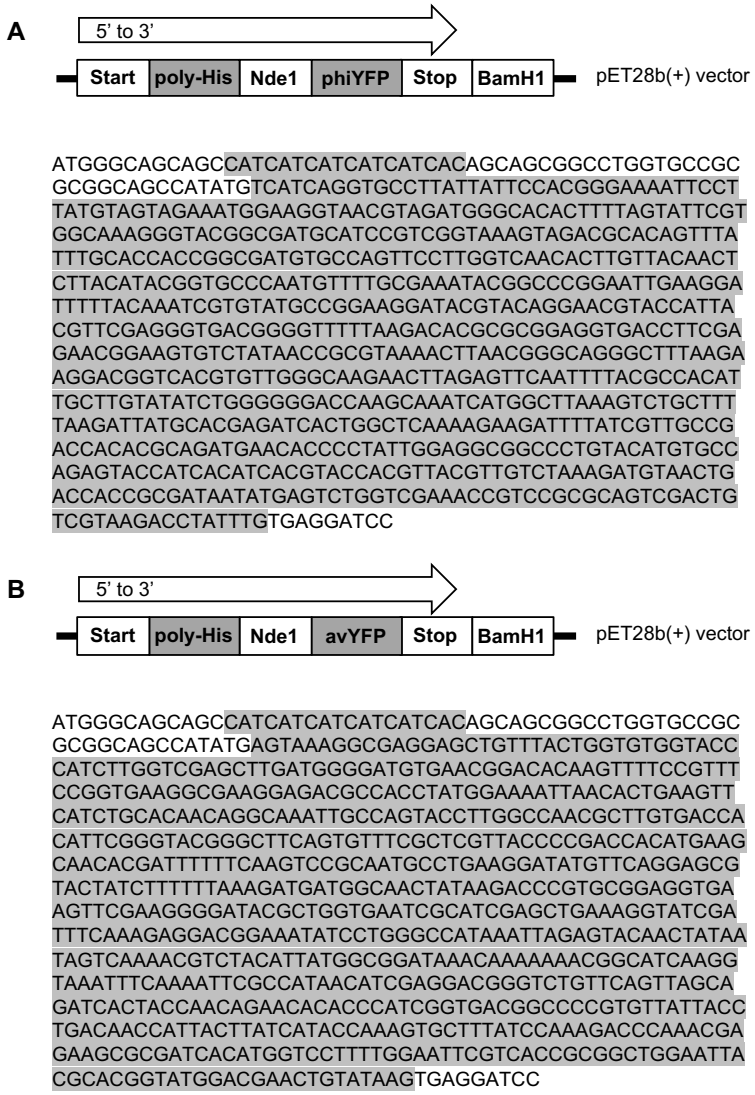

Figure S23. The nucleotide sequences for (A) phiYFP and (B) avYFP-H148Q used in this study. The genes were cloned in the pET-28b(+) vector between the Nde1 and BamH1 restriction sites with an N-terminal polyhistidine-tag.

Table S2. List of the primers used to generate the phiYFP Q69 site-saturation mutagenesis library.

Description	Sequence (5' to 3')
Q69 SSM Forward	ACTCTTACATACGGTGCCNDTTGTTTTGCGAAATACG
	ACTCTTACATACGGTGCCVHGTGTTTTGCGAAATACG
	ACTCTTACATACGGTGCCTGGTGTTTTGCGAAATACG
Reverse Primer	GGCACCGTATGTAAGAGTTGTAACAAGTGTTGAC

Table S3. Polymerase chain reaction conditions used to generate the phiYFP Q69 site-saturation mutagenesis library.

Step	Temp. (ºC)	Time (s)	Cycle No.
Template Denaturation	95	30	1
	95	10	30
Annealing	54.5	30	
Short Extenstion	72	240	
Long Extension	72	600	1
Storage	10	∞	1

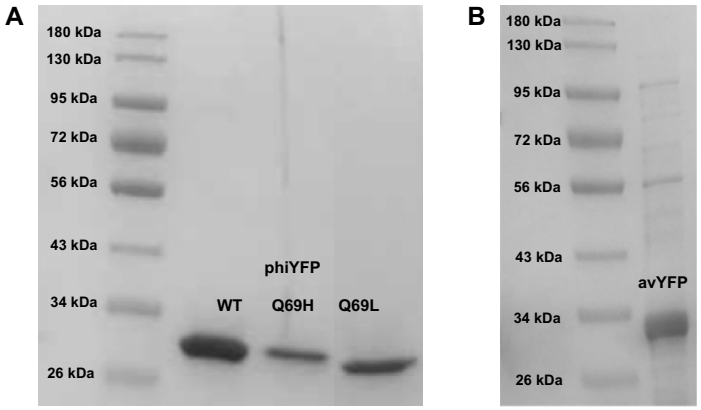

Figure S24. Coomassie stained SDS-PAGE gels of (A) the purified wild-type phiYFP, phiYFP Q69H, and phiYFP Q69L proteins and (B) the purified avYFP-H148Q.

REFERENCES

(1) McWilliam, H., Li, W., Uludag, M., Squizzato, S., Park, Y. M., Buso, N., Cowley, A. P., and Lopez, R. (2013) Analysis Tool Web Services from the EMBL-EBI. *Nucleic Acids Res. 41*, W597–W600.

(2) Kille, S., Acevedo-Rocha, C. G., Parra, L. P., Zhang, Z., Opperman, D. J., Reetz, M. T., and Acevedo, J. P. (2013) Reducing codon redundancy and screening effort of combinatorial protein libraries created by saturation mutagenesis. *ACS Synth. Bio*l. *2*, 83–92.

(3) Engqvist, M. K. M., McIsaac, R. S., Dollinger, P., Flytzanis, N. C., Abrams, M., Schor, S., and Arnold, F. H. (2015) Directed evolution of Gloeobacter violaceus Rhodopsin spectral properties. *J. Mol. Biol. 427*, 205–220.

(4) Hill, A. V. (1910) The heat produced in contracture and muscular tone. *J. Physiol. 40*, 389-403.

(5) Rurack, K. and Spieles, M. (2011) Fluorescence quantum yields of a series of red and near-infrared dyes emitting at 600-1000 nm. *Anal. Chem. 83*, 1232–1242.

(6) Magde, D., Wong, R., and Seybold, P. G. (2002) Fluorescence quantum yields and their relation to lifetimes of rhodamine 6G and fluorescein in nine solvents: improved absolute standards for quantum yields. *Photochem. Photobiol. 75*, 327–34.

(7) Kozma, I. Z., Krok, P., and Riedle, E. (2005) Direct measurement of the group-velocity mismatch and derivation of the refractive-index dispersion for a variety of solvents in the ultraviolet. *J. Opt. Soc. Am. B 22*, 1479–1485.

(8) Hale, G. M. and Querry, M. R. (1973) Optical constants of water in the 200-nm to 200-μm wavelength region. *Appl. Opt. 12*, 555–563.